Journal of Inorganic Biochemistry 236 (2022) 111952

Contents lists available at ScienceDirect

Journal of Inorganic Biochemistry

journal homepage: www.elsevier.com/locate/jinorgbio

Inhibition of SERCA and PMCA Ca^{2+}-ATPase activities by polyoxotungstates

Manuel Aureliano [a,b,*], Gil Fraqueza [b,c], Maria Berrocal [d,e], Juan J. Cordoba-Granados [d], Nadiia I. Gumerova [f], Annette Rompel [f,**], Carlos Gutierrez-Merino [d,e], Ana M. Mata [d,e,***]

[a] FCT, Universidade do Algarve, 8005-139 Faro, Portugal
[b] CCMar, Universidade do Algarve, 8005-139 Faro, Portugal
[c] ISE, Universidade do Algarve, 8005-139 Faro, Portugal
[d] Departamento de Bioquímica y Biología Molecular y Genética, Facultad de Ciencias, Universidad de Extremadura, 06006 Badajoz, Spain
[e] Instituto de Biomarcadores de Patologías Moleculares, Universidad de Extremadura,06006 Badajoz, Spain
[f] Universität Wien, Fakultät für Chemie, Institut für Biophysikalische Chemie, 1090 Vienna, Austria

ARTICLE INFO

Keywords:
Polyoxometalates
Polyoxometalate's stability
Ca^{2+}-ATPase
ATPases inhibitors
Anticancer drugs
Drug discovery

ABSTRACT

Plasma membrane calcium ATPases (PMCA) and sarco(endo) reticulum calcium ATPases (SERCA) are key proteins in the maintenance of calcium homeostasis. Herein, we compare for the first time the inhibition of SERCA and PMCA calcium pumps by several polyoxotungstates (POTs), namely by Wells-Dawson phosphotungstate anions $[P_2W_{18}O_{62}]^{6-}$ (intact, $\{P_2W_{18}\}$), $[P_2W_{17}O_{61}]^{10-}$ (monolacunary, $\{P_2W_{17}\}$), $[P_2W_{15}O_{56}]^{12-}$ (trilacunary, $\{P_2W_{15}\}$), $[H_2P_2W_{12}O_{48}]^{12-}$ (hexalacunary, $\{P_2W_{12}\}$), $[H_3P_2W_{15}V_3O_{62}]^{6-}$ (trivanadium-substituted, $\{P_2W_{15}V_3\}$) and by Preyssler-type anion $[NaP_5W_{30}O_{110}]^{14-}$ ($\{P_5W_{30}\}$). The speciation in the solutions of tested POTs was investigated by ^{31}P and ^{51}V NMR spectroscopy. The tested POTs inhibited SERCA Ca^{2+}-ATPase activity, whereby the Preyssler POT showed the strongest effect, with an IC_{50} value of 0.37 μM. For $\{P_2W_{17}\}$ and $\{P_2W_{15}V_3\}$ higher IC_{50} values were determined: 0.72 and 0.95 μM, respectively. The studied POTs showed to be more potent inhibitors of PMCA Ca^{2+}-ATPase activity, with lower IC_{50} values for $\{P_2W_{17}\}$, $\{P_5W_{30}\}$ and $\{P_2W_{15}V_3\}$.

1. Introduction

Polyoxometalates (POMs) are a well-known group of anionic polynuclear oxometals consisting typically of five forming elements V^V, Ta^V, Nb^V, W^{VI} and Mo^{VI} with distinct and chemically changeable structures [1]. In addition, POMs structures can include other elements such as non-metals (e. g. P^V, As^V, Si^{IV}) and one or more of the addenda metal-oxo fragments may be absent and/or substituted by transition metal ions (e. g. Fe^{III}, Co^{II}, Ni^{II}). Due to POMs' diversity they have shown specific physicochemical properties responsible for discrete chemical and biological applications such as catalysis, protein crystallization, anticancer, antibacterial and antidiabetic activities, among others [2,3,4,5,6,7,8,9].

The biological and pharmacological action of POMs is often related to their inhibition of enzymes such as aquaporin's [10], phosphatases [11], polyphenol oxidases [12], glucosidases [13] and P-type ATPases [14]. Among them, the P-type ATPases, Na^+/K^+-ATPase and Ca^{2+}-ATPase, represent important biological targets which is reflected by the substantial number of drugs targeting these ion pumps [15]. Since 1991,

Abbreviations: ATPase, Adenosine triphosphatase; BMOV, Bismaltol oxidovanadium(IV); CPA, Cyclopyazonic acid; IC_{50}, Half maximal inhibitory concentration; IU, International Units; PMCA, Plasmatic membrane calcium ATPase; POMs, Polyoxometalates; POTs, Polyoxotungstates; SERCA, Sarco(endo) plasmatic membrane calcium ATPase; SR, Sarcoplasmic reticulum; TG, Thapsigargin; POVs, Polyoxovanadates; HEPES, 4-(2-hydroxyethyl)-1-piperazineethanesulfonic acid; P_2W_{12}, $[H_2P_2W_{12}O_{48}]^{12-}$; P_2W_{15}, $[P_2W_{15}O_{56}]^{12-}$; P_2W_{17}, $[P_2W_{17}O_{61}]^{10-}$; P_2W_{18}, $[P_2W_{18}O_{62}]^{6-}$; $P_2W_{15}V_3$, $[H_3P_2W_{15}V_3O_{62}]^{6-}$; P_5W_{30}, $[NaP_5W_{30}O_{110}]^{14-}$; EDTA, ethylenediaminetetraacetic acid; V_{10}, decavanadate; Nb_{10}, decaniobate.

* Correspondence to: M. Aureliano, FCT, Universidade do Algarve, 8005-139 Faro, Portugal
** Correspondence to: A. Rompel, Universität Wien, Fakultät für Chemie, Institut für Biophysikalische Chemie, 1090 Vienna, Austria
*** Correspondence to: A. M. Mata, Departamento de Bioquímica y Biología Molecular y Genética, Facultad de Ciencias, Universidad de Extremadura, 06006 Badajoz, Spain
E-mail addresses: maalves@ualg.pt (M. Aureliano), annette.rompel@univie.ac.at (A. Rompel), anam@unex.es (A.M. Mata).

https://doi.org/10.1016/j.jinorgbio.2022.111952
Received 26 May 2022; Received in revised form 20 July 2022; Accepted 27 July 2022
Available online 31 July 2022
0162-0134/© 2022 The Authors. Published by Elsevier Inc. This is an open access article under the CC BY license (http://creativecommons.org/licenses/by/4.0/).

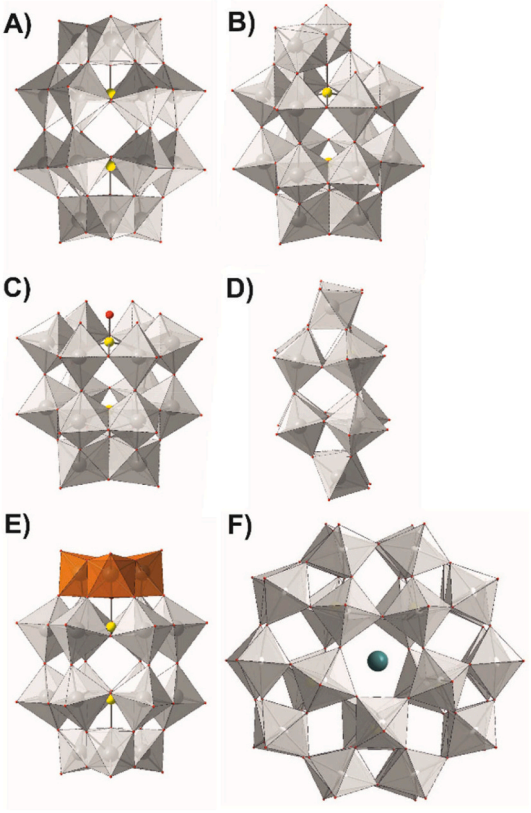

Fig. 1. POT structures tested in this study: A) intact Wells-Dawson anion $[P_2W_{18}O_{62}]^{6-}$ ($\{P_2W_{18}\}$); B) monolacunary Wells-Dawson anion $[P_2W_{17}O_{61}]^{10-}$ ($\{P_2W_{17}\}$); C) trilacunary Wells-Dawson anion $[P_2W_{15}O_{56}]^{12-}$ ($\{P_2W_{15}\}$); D) hexalacunary Wells-Dawson anion $[H_2P_2W_{12}O_{48}]^{12-}$ ($\{P_2W_{12}\}$); E) trivanadium-substituted Wells-Dawson anion $[H_3P_2W_{15}V_3O_{62}]^{6-}$ ($\{P_2W_{15}V_3\}$); F) Preyssler anion $[NaP_5W_{30}O_{110}]^{14-}$ ($\{P_5W_{30}\}$). Color code: $\{WO_6\}$, grey; $\{VO_6\}$, orange; P, yellow; O, red; Na, teal blue. (For interpretation of the references to color in this figure legend, the reader is referred to the web version of this article.)

Aureliano and coworkers worked extensively on in vitro and in vivo interactions of POMs, particularly polyoxovanadates (POVs) and polyoxotungstates (POTs), with these membrane proteins and recently also with aquaporin's on diverse biochemical processes that will explain POMs actions on biomedicinal applications against iter alia anticancer, antibacterial and/or viral infections. [6,7,8,16,17,18,19,20–22]

It has been suggested that due to their large size, POMs such as decavanadate exert their actions outside the cell by targeting P-type ATPases [23]. In fact, a putative mechanism of POMs' action in biological systems can involve, among others, the interaction with membrane proteins such as ion pumps [7,8,14,16,21], aquaporin's [10] as well as hormone receptors, as recently referred, inducing directly or indirectly activation of signaling processes [24]. Regarding POTs, very little or even nothing is known about the POTs inhibitory capacity on plasmatic membrane calcium ATPase (PMCA) Ca^{2+}-ATPase activity. This prompted us to further pursue the investigation of the effects of the Wells-Dawson (Fig. 1A) and the Preyssler POT archetypes (Fig. 1F) on the sarco(endo) reticulum calcium ATPase (SERCA) Ca^{2+}-ATPase activity localized at the sarcoplasmic or endoplasmic reticulum, already used as a model for the study with others POTs [21], and on the activity of the PMCA Ca^{2+}-ATPase localized at the plasmatic membrane, that to ours knowledge has never been studied before.

Here, we report and compare effects of six POTs: Wells-Dawson phosphotungstate anions $[P_2W_{18}O_{62}]^{6-}$ (intact, {abbreviated P_2W_{18}}), $[P_2W_{17}O_{61}]^{10-}$ (monolacunary, $\{P_2W_{17}\}$), $[P_2W_{15}O_{56}]^{12-}$ (trilacunary, $\{P_2W_{15}\}$), $[H_2P_2W_{12}O_{48}]^{12-}$ (hexalacunary, $\{P_2W_{12}\}$), $[H_3P_2W_{15}V_3O_{62}]^{6-}$ (trivanadium-substituted, $\{P_2W_{15}V_3\}$) and by Preyssler type anion $[NaP_5W_{30}O_{110}]^{14-}$ ($\{P_5W_{30}\}$) (Table 1), on SERCA Ca^{2+}-ATPase activity, obtained from skeletal muscle, and on the pig brain PMCA Ca^{2+}-ATPase activity. Thus, the aims of the present study are: i) to test and compare the extent of inhibition of six polyoxotungstates against SERCA and PMCA Ca^{2+}-ATPase activities; ii) to compare their inhibitory capacity with other POTs and POMs as well as other metal compounds and well-known drugs that target these key P-type ATPases on cellular ion homeostasis; iii) to characterize and compare the POTs type of Ca^{2+}-ATPase inhibition relative to the protein's native substrate MgATP; iv) to analyze the POTs's speciation and stability under experimental conditions; v) to correlate the inhibitory capacity with structural features of the investigated POTs.

2. Materials and methods

2.1. Polyoxotungstates

The POTs used in this study are summarized in Table 1, were synthesized according to published procedures and their purity was confirmed by infrared (Fig. S1, Table S1), ^{31}P and ^{51}V NMR spectroscopy (Figs. 6 and 7, Fig. S2-S5). The POTs' stock solutions were freshly

Table 1
POTs used in this study.

Sum Formula	Molar weight	Net charge	Charge density (charge / number of addenda atoms ratio)	First structural report in	Synthesis	pH in 1 mM POM aqueous solution / Anions present in aqueous solution[a]	pH in 1 mM POM in HEPES[b] 7.0 buffer solution / Anions present in HEPES[b] 7.0 buffer
$K_6[\alpha\text{-}P_2^VW_{18}^{VI}O_{62}]\cdot 14H_2O$ $\{P_2W_{18}\}$	4849.6	−6	0.33	[25]	[26]	pH 5.9 / $[\alpha\text{-}P_2W_{18}O_{62}]^{6-}$ (Fig. S2A)	pH 6.2 / $[\alpha\text{-}P_2W_{18}O_{62}]^{6-}$ + $[\alpha_2\text{-}P_2W_{17}O_{61}]^{10-}$ (Fig. S2B)
$K_{10}[P_2W_{17}O_{61}]\cdot 20H_2O$ $\{P_2W_{17}\}$	4914.2	−10	0.56	[27]	[26]	pH 7.1 / $[\alpha_2\text{-}P_2W_{17}O_{61}]^{10-}$ (Fig. S3A)	pH 6.9 / $[\alpha_2\text{-}P_2W_{17}O_{61}]^{10-}$ (Fig. S3B)
$Na_{12}[P_2W_{15}O_{56}]\cdot 24H_2O$ $\{P_2W_{15}\}$	4423.8	−12	0.80	[28]	[26]	pH 9.9 / $[\alpha_2\text{-}P_2W_{17}O_{61}]^{10-}$ (Fig. S4A)	pH 7.1 / $[\alpha_2\text{-}P_2W_{17}O_{61}]^{10-}$ (Fig. S4B)
$(NH_4)_{12}[H_2P_2W_{12}O_{48}]\cdot 24H_2O$ $\{P_2W_{12}\}$	3686.8	−12	1.00	[29]	[26]	pH 6.2 / $[\alpha_2\text{-}P_2W_{17}O_{61}]^{10-}$ + $[P_2W_{19}O_{69}(H_2O)]^{14-}$ + $[H_2P_2W_{12}O_{48}]^{12-}$ (Fig. S5A)	pH 6.7 / $[\alpha_2\text{-}P_2W_{17}O_{61}]^{10-}$ + $[P_2W_{19}O_{69}(H_2O)]^{14-}$ + $[H_2P_2W_{12}O_{48}]^{12-}$ (Fig. S5B)
$[N(CH_3)_4]_6[H_3P_2W_{15}V_3O_{62}]\cdot 6H_2O$ $\{P_2W_{15}V_3\}$	4372.0	−6	0.33	[30]	[30]	pH 2.2 / $[H_3P_2W_{15}V_3O_{62}]^{6-}$ (Fig. 7A)	pH 5.7 / $[H_3P_2W_{15}V_3O_{62}]^{6-}$ (Fig. 7B)
$(NH_4)_{14}[NaP_5W_{30}O_{110}]\cdot 31H_2O$ $\{P_5W_{30}\}$	8264.0	−14	0.47	[31]	[32]	pH 3.5 / $[NaP_5W_{30}O_{110}]^{14-}$ (Fig. 6A)	pH 7.2 / $[NaP_5W_{30}O_{110}]^{14-}$ (Fig. 6B)

[a] Speciation was studied by ^{31}P and ^{51}V NMR spectroscopy.
[b] The exact composition of buffer is 25 mM HEPES (pH 7.0), 100 mM KCl, 5 mM $MgCl_2$, 50 μM $CaCl_2$. All solutions were incubated for 30 min at 37 °C to simulate biological conditions.

prepared by dissolving the solid compound in water. The pH values of the aqueous POTs solutions varied from 2 to 5, and are also dependent on the concencentration of each POT solution. The concentrations of the stock solutions used were 10 mM and/or 1 mM, depending on solubility and enzymatic inhibitory capacity. For solution stability studies ^{31}P and ^{51}V NMR spectroscopy was used. ^{31}P NMR spectra were recorded with a Bruker FT-NMR spectrometer Avance Neo 500 MHz (Bruker, Rheinstetten, Germany) at 25 °C and 202.53 MHz. The chemical shifts were measured relative to 85% H_3PO_4 ($\delta = 0$ ppm). ^{51}V NMR spectra were performed on a Bruker Avance II 500 MHz (Bruker, Rheinstetten, Germany) instrument operating at 25 °C and 131.60 MHz (2000 scans, accumulation time 0.05 s, relaxation delay 0.01 s). Chemical shift values are given with reference to $VOCl_3$ ($\delta = 0$ ppm) as a standard.

2.2. Preparation of sarcoplasmic reticulum Ca^2 -ATPase (SERCA) vesicles

The sarcoplasmic reticulum (SR) Ca^{2+} -ATPase vesicles were isolated from rabbit skeletal muscles as described elsewhere [21,22,33,34] suspended in 0.1 M KCl, 10 mM 4-(2-hydroxyethyl)-1-piperazineethanesulfonic acid (HEPES) pH 7.0, diluted 1:1 with 2.0 M sucrose and frozen in liquid nitrogen for storage at −80 °C. The protein concentration was determined by Bradford method at 595 nm [35], in the presence of 0.125% of sodium dodecyl sulphate. As analyzed by SDS-PAGE the sarcoplasmic reticulum Ca^{2+}-ATPase-1 (SERCA-1) was the predominant isoform in our SR preparations. The rabbit SR protocols were performed under a “Group C" license from the Direcção-Geral de Veterinária, Ministério da Agricultura, do Desenvolvimento Rural e das Pescas, Portugal.

2.3. Effects of POTs on SERCA activity

SERCA Ca^{2+}-ATPase activities were measured spectrophotometrically at room temperature (22 °C) using the coupled enzyme pyruvate kinase/lactate dehydrogenase assay, as described elsewhere [20,22]. The following medium conditions were used: 25 mM HEPES (pH 7.0), 100 mM KCl, 5 mM $MgCl_2$, 50 μM $CaCl_2$, 2.5 mM ATP. For the coupled enzyme assay 0.42 mM phosphoenolpyruvate, 0.25 mM NADH, 18 IU lactate dehydrogenase and 7.5 IU pyruvate kinase, were added to the medium. The experiments were initiated by the addition of 10 μg/ml SERCA, and followed for 3 min, as briefly described below. Freshly prepared POTs solutions were added to the medium referred above immediately prior to sarcoplasmic reticulum Ca^{2+}-ATPase vesicles addition. After the addition of the enzyme, the absorbance at 340 nm was recorded for about 1 minute (basal activity) and then 4% (*w*/w) of calcium ionophore A23187 was added to the cuvette and the decrease in absorbance was measured for 2 minutes (uncoupled ATPase activity). The ATPase activity and the inhibition were measured taken into consideration the decrease in absorbance per minute in the absence (100%) and in the presence of the inhibitor under the applied condition of uncoupled ATPase activity, as described elsewhere [20,21,22]. All experiments were performed at least in triplicate. The inhibitory power of the investigated POTs was evaluated by determining IC_{50} values (POTs concentration inducing 50% of Ca^{2+}-ATPase activity inhibition).

2.4. Effects of POTs on PMCA activity

2.4.1. Preparation of purified synaptosomal PMCA

The PMCA was purified from pig brain (obtained from a local slaughterhouse), as described by Salvador and Mata [36]. Briefly, fresh cerebrum (~80 g) obtained from a local slaughterhouse, was homogenized in 10 vol of 10 mM HEPES/KOH, pH 7.4; 0.32 M sucrose; 0.5 mM $MgSO_4$; 0.1 mM phenylmethylsulfonyl fluoride; and 2 mM 2-mercaptoethanol. After two centrifugation steps at 1500×*g* and 20,000×g, the pellet was subjected to 40–20% (*w*/*v*) discontinuous sucrose gradient, and synaptosomes were obtained at the interface and resuspended in 10 mM HEPES/KOH, pH 7.4, and 0.32 M sucrose. Synaptosomes were lysed to obtain synaptosomal plasma membranes that were further solubilized with 0.6% (w/v) Triton X-100 and loaded onto a calmodulin affinity column. The fraction containing PMCA was eluted free of lipids with a buffer containing 15% glycerol, 0.06% Triton X-100, and 2 mM EDTA.

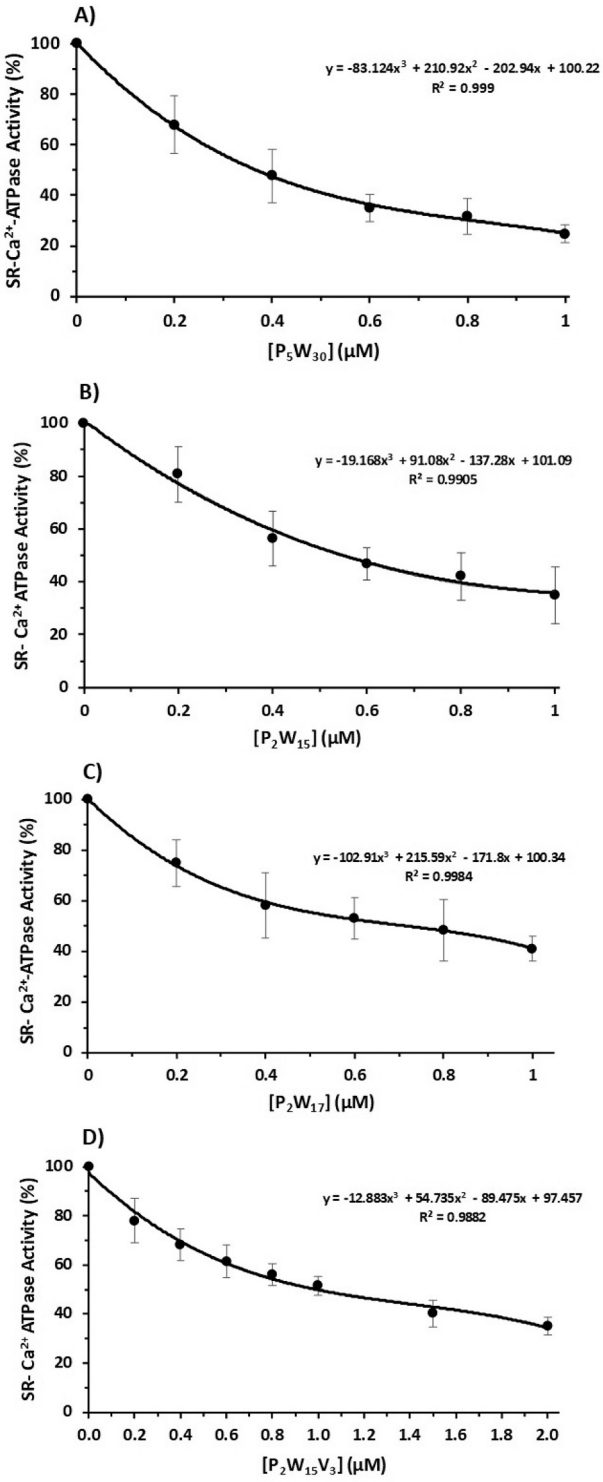

Fig. 2. Inhibition of SERCA Ca^{2+}-ATPase activity by POTs: A) $\{P_5W_{30}\}$; B) $\{P_2W_{15}\}$; C) $\{P_2W_{17}\}$; D) $\{P_2W_{15}V_3\}$, that was measured spectrophotometrically at 340 nm and 25 °C, using the coupled enzyme pyruvate kinase/lactate dehydrogenase assay. The experiments were initiated after the addition of 10 μg/mL calcium ATPase. Data are plotted as means ± SD. The results shown are the average of triplicate experiments.

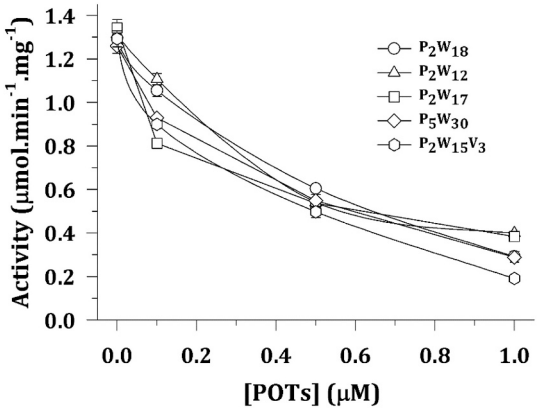

Fig. 3. Inhibition of PMCA Ca^{2+}-ATPase activity by POTs. The activity was measured spectrophotometrically at 340 nm and 37 °C, using the coupled enzyme pyruvate kinase/lactate dehydrogenase assay, as describe in the Methods, using 2.5 μg/mL of purified protein. The experiments were initiated after the addition of 1 mM ATP and subsequent additions of increasing concentration of the indicated POTs. Data are plotted as means ± SD. The results shown are the average of triplicate experiments.

The protein concentration was determined by the Bradford method [35].

2.4.2. PMCA Ca^{2+}-ATPase activity

Steady-state assays of the PMCA activity were measured spectrophotometrically at 37 °C, using the coupled enzyme pyruvate kinase/lactate dehydrogenase assay, as described elsewhere [37], under the following conditions: 50 mM HEPES (pH 7.4), 100 mM KCl, 2 mM $MgCl_2$, 5 mM NaN_3, 3.16 μM free Ca^{2+}, 0.42 mM phosphoenolpyruvate, 0.22 mM NADH, 28 IU lactate dehydrogenase and 10 IU pyruvate kinase. Briefly, delipidated purified PMCA (2.5 μg) containing 0.06% Triton X-100 was mixed with 13.32 μg of phosphatidylcholine type IIS (PCIIS, from Sigma) previously dried under a N_2 atmosphere. The mixture was incubated for 2 min at 37 °C and then diluted to 1 ml assay medium. Activities were measured after subsequent additions of 1 mM ATP (to start the reaction) and increasing concentrations of POTs [37,38]. All experiments were performed at least in triplicate and with three different preparations.

2.5. Statistical analysis

Calculations of IC_{50} values were performed using Microsoft Office 365 Excel (2019) (Microsoft, Redmond, WA, USA). All values shown are presented as averages and standard deviations of measurements taken from triplicate measurements, using three distinct and independent Ca^{2+}-ATPase preparations. The statistical significance of the data was assessed using the Student's *t*-test. Differences from controls were considered significant at $p < 0.05$.

3. Results and discussion

3.1. Inhibition of SERCA activity by POTs

In the present study, we explore the inhibitory potential of POTs regarding the SERCA Ca^{2+}-ATPase inhibition previously described [21] and we are now continuing the studies using others POTs. All the investigated POTs inhibited Ca^{2+}-ATPase activity, which is expressed as percentage of the control enzymatic activity value obtained without inhibitor, in a concentration dependent manner (Fig. 2). The Preyssler anion $\{P_5W_{30}\}$ showed a higher potency to inhibit the SERCA Ca^{2+}-ATPase activity with IC_{50} values of 0.37 μM (Fig. 2), while the Well–Dawson POTs, $\{P_2W_{15}\}$, $\{P_2W_{17}\}$ and $\{P_2W_{15}V_3\}$ showed higher IC_{50} values: 0.55, 0.72 and 0.95 μM, respectively (Fig. 2).

Table 2
SERCA and PMCA IC_{50} values of Ca^{2+}-ATPase inhibition by POTs. SERCA values for $\{P_2W_{12}\}$ and $\{P_2W_{18}\}$ were previously determined [21]. n.d. is not dertermined.

POT	IC_{50} (μM)	
	SERCA	PMCA
$\{P_2W_{18}\}$	0.60 [21]	0.30
$\{P_2W_{17}\}$	0.72	0.10
$\{P_2W_{15}\}$	0.55	n.d.
$\{P_2W_{12}\}$	11.0 [21]	0.25
$\{P_2W_{15}V_3\}$	1.00	0.23
$\{P_5W_{30}\}$	0.37	0.18

Note that the compounds were added to the medium seconds before the reaction was initiated. Moreover, following the addition of POTs, the rates of the reactions in the presence of different inhibitor concentrations were measured within the following 2–3 min. While $\{P_5W_{30}\}$, $\{P_2W_{15}V_3\}$ and $\{P_2W_{17}\}$ remain intact under experimental conditions (Figs. 6 and 7), $\{P_2W_{18}\}$ partially hydrolyzes into monolacunary anions, $\{P_2W_{15}\}$ rearranged into monolacunary species, and in solution of $\{P_2W_{12}\}$, mixture of hexalacunary, monolacunary and $[P_2W_{19}O_{69}(H_2O)]^{14-}$ anions are present (Figs. 6 and 7, Fig. S2-S5, see more details in section 3.6). Therefore, the inhibitory effects determined can be deduce to the POTs added to the reaction medium.

3.2. Inhibition of PMCA activity by POTs

The effects of five POTs on the activity of the purified PMCA were investigated. The POTs were added to the assay after triggering the reaction with ATP, as indicated in the Materials and Methods section. As shown in Fig. 3, all the POTs studied; $\{P_2W_{17}\}$, $\{P_5W_{30}\}$, $\{P_2W_{15}V_3\}$, $\{P_2W_{12}\}$ and $\{P_2W_{18}\}$ inhibited the Ca^{2+}-ATPase activity of PMCA, in a concentration dependent manner. The inhibitory capacity of the investigated POTs compounds was evaluated by the half maximal inhibitory concentration (IC_{50}) values. The IC_{50} values were calculated using Microsoft Office 365 Excel (Microsoft, Redmond, WA, USA), and ranged from 0.10 ± 0.01 μM to 0.32 ± 0.01 μM. The POTs $\{P_2W_{17}\}$ and $\{P_5W_{30}\}$ showed higher inhibitory capacity with the lowest determined IC_{50} values: 0.10 and, 0.17 μM, respectively, whereas the others 3 POTs $\{P_2W_{15}V_3\}$, $\{P_2W_{12}\}$ and $\{P_2W_{18}\}$ showed IC_{50} values around 0.3 μM (Table 2).

Thus, the studied POTs with high affinity for these P-type ATPases can be observed to be more potent inhibitors of PMCA Ca^{2+}-ATPase activity, once lower IC_{50} values for $\{P_2W_{17}\}$, $\{P_5W_{30}\}$ and $\{P_2W_{15}V_3\}$ were received: 0.10 (×7 fold lower), 0.17 (×2 fold lower) and 0.25 μM (×4 fold lower), respectively, compared to SERCA Ca^{2+}-ATPase inhibition (Table 2).

3.3. SERCA and PMCA inhibitory potential of POTs, inorganic and organic compounds

Indeed, in previous SERCA Ca^{2+}-ATPase studies, using exactly the same experimental conditions as in the present study, Ca^{2+}-ATPase IC_{50} inhibition values below 1 μM, have previously been determined for others POTs, such as intact Wells-Dawson anion $[P_2W_{18}O_{62}]^{6-}$ $\{P_2W_{18}\}$ (0.6 μM) and $\{Se_2W_{29}\}$ (IC_{50} = 0.3 μM) [21]. IC_{50} values for P-type ATPase inhibitory activity of POMs ranging from 1 to 35 μM, have been determined for decaniobate $[Nb_{10}O_{28}]^{6-}$ $\{Nb_{10}\}$ (IC_{50} = 35 μM), Keggin-based POTs such as mono-substituted $\{CoW_{11}\}$ (IC_{50} = 4 μM), trilacunary $\{SiW_9\}$ (IC_{50} = 16 μM) and $\{AsW_9\}$ (20 μM), lacunary Dawson type $\{P_2W_{12}\}$ (11 μM), and also for $\{As_2W_{19}\}$ (28 μM) [21]. Regarding POVs, IC_{50} values ranging from 5 to 35 μM, were also determined for $\{PV_{14}\}$ (IC_{50} = 5 μM) and for $\{MnV_{13}\}$ (IC_{50} = 31 μM) [22,33]. Lower inhibitory potency was also determined for some POVs and POTs, such as for $\{MnV_{11}\}$ (IC_{50} = 58 μM) and for $\{TeW_6\}$ (IC_{50} = 200 μM) [21,33].

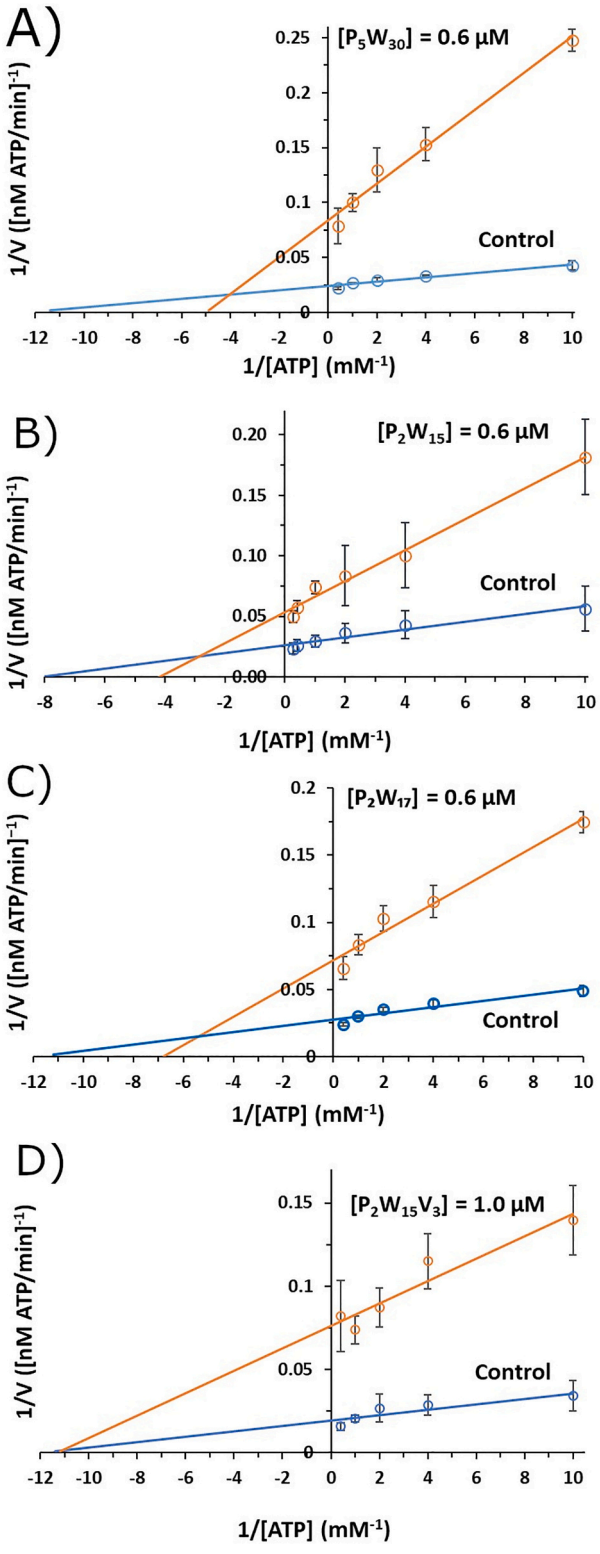

Fig. 4. Lineweaver-Burk plots of SERCA Ca^{2+}-ATPase activity in the absence (blue) and in the presence (orange) of POTs. A) $\{P_5W_{30}\}$; B) $\{P_2W_{15}\}$; C) $\{P_2W_{17}\}$; D) $\{P_2W_{15}V_3\}$. The plots were used for determining the type of enzyme inhibition. Data are plotted as means ± SD. The results shown are the average of triplicate experiments. (For interpretation of the references to colour in this figure legend, the reader is referred to the web version of this article.)

Further studies with SERCA Ca^{2+}-ATPase, described that besides POVs, such as decavanadate $\{V_{10}\}$ (IC_{50} = 15 μM), monomeric vanadate $\{V_1\}$ (IC_{50} = 80 μM), monomeric tungstate (IC_{50} = 400 μM), oxidovanadium compounds such as bis(maltolato)oxovanadium(IV) (BMOV) (IC_{50} = 80 μM), and very recently gold compounds (IC_{50} = 0.4–16.3 μM) are also SERCA Ca^{2+}-ATPase inhibitors [20,34,39]. In the present study, the PMCA IC_{50} value of inhibition for decavanadate (50 μM) was also determined, which was 3 times higher than the one referred for SERCA.

Table 3
K_m and V_{max} values of SERCA Ca^{2+}-ATPase inhibition by POTs.

POT		K_m (mM)	V_{max} (nM ATP·min^{-1})	Type of inhibition
$\{P_2W_{15}\}$	0 (μM)	0.122 ± 0.014[a]	38.02 ± 6.85[a]	Mixed
	0.6 (μM)	0.239 ± 0.021[b]	18.69 ± 3.31[b]	
$\{P_2W_{17}\}$	0 (μM)	0.084 ± 0.011[c]	36.50 ± 7.38[a]	Mixed
	0.6 (μM)	0.146 ± 0.015[d]	13.91 ± 2.32[c]	
$\{P_5W_{30}\}$	0 (μM)	0.079 ± 0.016[e]	41.32 ± 8.87[a]	Mixed
	0.6 (μM)	0.200 ± 0.018[f]	11.95 ± 1.78[d]	
$\{P_2W_{15}V_3\}$	0 (μM)	0.104 ± 0.020[g]	53.24 ± 3.38[e]	non-competitive
	1.0 (μM)	0.097 ± 0.020[g]	14.52 ± 1.25[e]	

[a-g]Averages ± S.D. in same column with different letters are significantly different (p<0.05).

Ouabain, omeprazole, thapsigargin (TG) and cyclopiazonic acid (CPA) are such drugs as SERCA Ca^{2+}-ATPase inhibitors. Several ranges of IC_{50} values can be found among these drugs for instance thapsigargin (IC_{50} = 0.001–0.029 μM), cyclopiazonic acid (IC_{50} = 0.1–0.2 μM), macrocyclic lactones (IC_{50} = 66–72 μM), and curcuminoides (IC_{50} = 7–17 μM) among others [40,41,42,43,44]. These organic inhibitors of the SERCA Ca^{2+}-ATPases are used for various disease treatments, such as heart failure, antipsychotic, anti-malaria and also as anaesthetics, tumour promoter, antibiotic and insulin mimetic agents [40,41,42,43,44]. Regarding the PMCA pump, polyamines, such as spermine [45] and the antipsychotic drug thioridazine [46] have been shown to inhibit it as well as by gold compounds [47]. Herein, POTs were found to inhibit the PMCA pump with IC_{50} values ranging 0.1–0.3 μM. When these POTs IC_{50} values are compared to those found for the organic compounds described above, it is clear that the inhibitory capacity for the POTs is much stronger with respect to the PMCA pump, i.e., some POT is at least >770 times more efficient.

3.4. POTs mode of inhibition of SERCA calcium ATPase activity

Herein, it was determined that the Preyssler anion $\{P_5W_{30}\}$, the trilacunary Wells-Dawson anion $\{P_2W_{15}\}$, the monolacunary Wells-Dawson anion $\{P_2W_{17}\}$ showed a mixed type inhibition, while the trivanadium-substituted Wells-Dawson $\{P_2W_{15}V_3\}$ presented a non-competitive type inhibition regarding SERCA ATPase activity (Fig. 4).

In fact, for the majority of the POTs studied, their V_{max} values decrease, compared to the control, while at the time the corresponding K_m values increase, which is typical for a mixed type inhibition (Table 3). Thus, it can be proposed that mixed type inhibition is observed for all POTs meaning that they interact with the Ca^{2+}-ATPase regardless whether or not the enzyme has already bound substrate, suggesting two different protein binding sites for all these POTs. However, it was observed that $\{P_2W_{15}V_3\}$ reduced the V_{max}, without affecting the K_m, therefore showing the effect of non-competitive inhibition, suggesting that the V3 site of the POM might contribute for a different mode of protein binding.

A mixed type inhibition, was also previously observed for others POTs and POVs, such as $\{P_2W_{18}\}$ and $\{PV_{14}\}$ [21,22]. In contrast decaniobate $\{Nb_{10}\}$ and decavanadate $\{V_{10}\}$ have previously been observed to be non-competitive inhibitors of Ca^{2+}-ATPase [22]. These

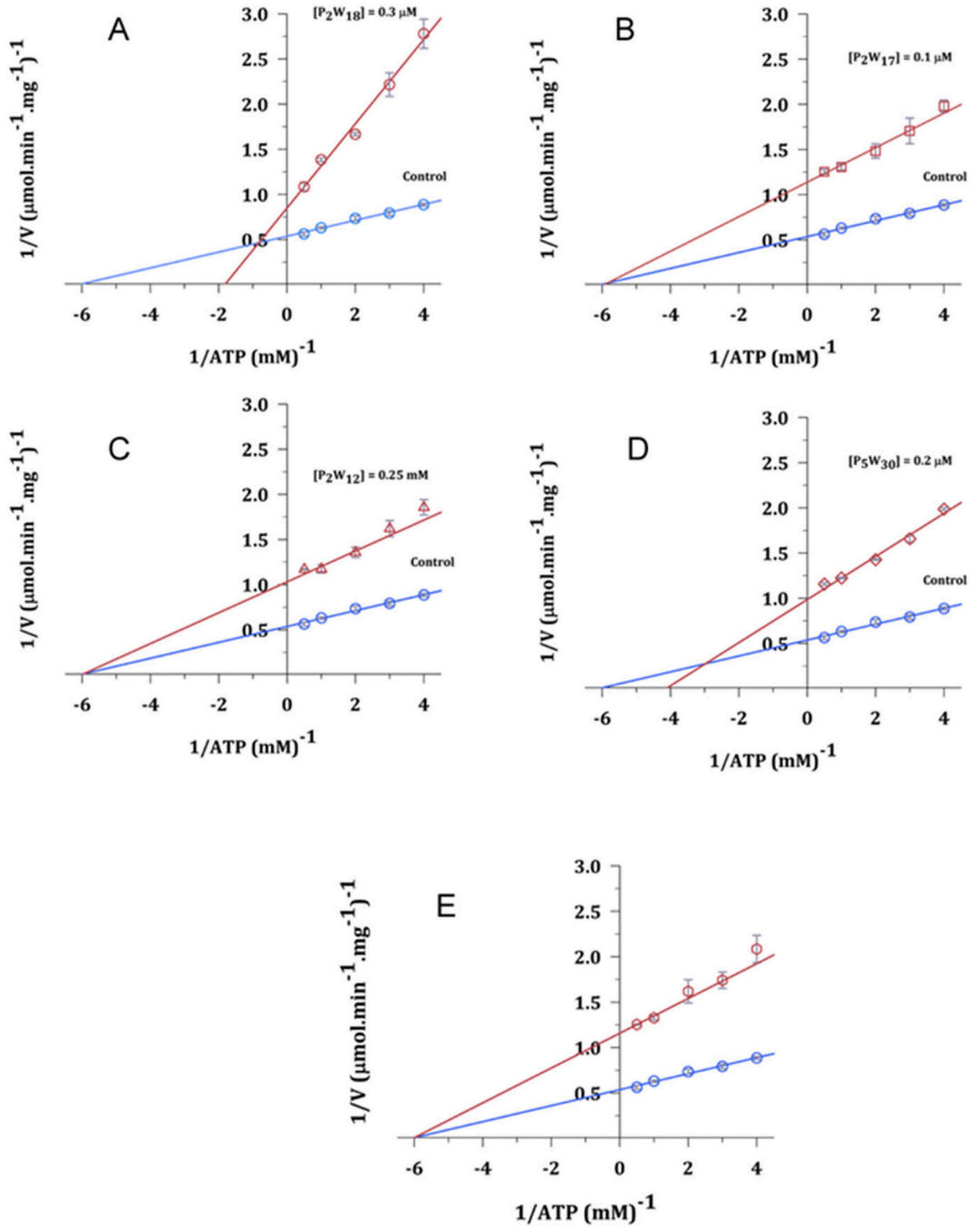

Fig. 5. Lineweaver-Burk plots of PMCA activity in the absence (blue symbols) and in the presence (red symbols) of POTs: A) $\{P_2W_{18}\}$; B) $\{P_2W_{17}\}$; C) $\{P_2W_{12}\}$; D) $\{P_5W_{30}\}$; E) $\{P_2W_{15}V_3\}$, at concentrations of 0.3, 0.1, 0.25, 0.2 and 0.25 μM, respectively. (For interpretation of the references to colour in this figure legend, the reader is referred to the web version of this article.)

observations suggest that several distinct POTs can interact with the Ca^{2+}-ATPase regardless of whether or not the enzyme has already bound substrate, and point to the existence of at least two different protein binding sites for these POTs, one of which is probably the ATP binding site. However, virtually nothing is known about the protein conformations favourable for interaction and binding sites for the interaction for most POMs with a few exceptions studying $\{V_{10}\}$ and $\{Nb_{10}\}$ interactions with Ca^{2+}-ATPase [17,20]. In these isopolyoxometalates studies, it was suggested that, $\{V_{10}\}$ could bind to all conformations either E1 or E2, phosphorylated or not, in contrast to vanadate, which only binds to E2 conformation of Ca^{2+}-ATPase. [20] Conversely, the mechanism of action and ATPases binding sites have been determined for some drugs such as thapsigargin (TG) and cyclopiazonic acid (CPA) [15].

For the determination of IC_{50} values, it was observed that after 30 min of incubation of all POTs in the medium, with or without the enzyme, the inhibition of the enzyme did not differ from that observed without incubation, suggesting that the compounds are stable at the experimental conditions used. However, speciation and stability studies were performed in the below section in order to deduce the POTs species present at the medium conditions used in the experiments described above.

Table 4
K_m, V_{max}, type of inhibition and IC_{50} values of PMCA inhibition by POTs compounds. *$P < 0.05$ vs control (without any compound).

POT compound (μM)		K_m (mM)	V_{max} (μmol·min^{-1}·mg^{-1})	Type of Inhibition	IC_{50} (μM)
	0	0.167 ± 0.008	1.88 ± 0.09		
{P_2W_{18}}	0.3	0.550 ± 0.02*	1.17 ± 0.05*	Mixed	0.3 ± 0.01
{P_2W_{12}}	0.25	0.166 ± 0.008	0.980 ± 0.05*	Non-competitive	0.25 ± 0.02
{P_2W_{17}}	0.1	0.168 ± 0.01	0.885 ± 0.04*	Non-competitive	0.1 ± 0.01
{P_5W_{30}}	0.2	0.244 ± 0.01*	1.03 ± 0.04*	Mixed	0.18 ± 0.02
{$P_2W_{15}V_3$}	0.25	0.164 ± 0.01	0.870 ± 0.04*	Non-competitive	0.23 ± 0.02

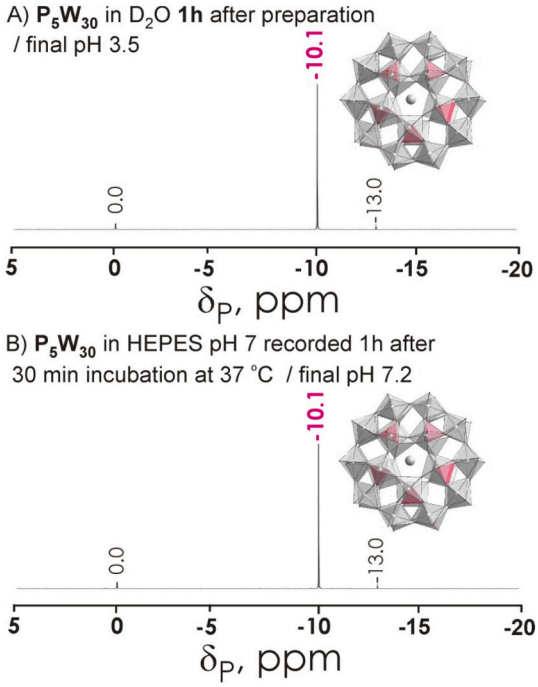

Fig. 6. ^{31}P NMR spectra of 10 mM {P_5W_{30}} solutions A) in D_2O recorded approximately 1 h after preparation; B) in 25 mM HEPES (pH 7.0), 100 mM KCl, 5 mM $MgCl_2$, 50 μM $CaCl_2$ recorded after incubation for 30 min at 37 °C. Signals at 0 ppm correspond to free phosphate $H_xPO_4^{(3-x)-}$ ($x = 0$–3). The signal at −10.1 ppm corresponds to 5 equivalent P ions in {P_5W_{30}} [32] shown in magenta in polyhedral presentation. Color code: {WO_6}, light grey; {PO_4}, magenta; O, red; Na, grey. (For interpretation of the references to color in this figure legend, the reader is referred to the web version of this article.)

3.5. POTs type of inhibition of PMCA calcium ATPase activity

The type of inhibition produced by the POTs compounds was analyzed at concentrations around the IC_{50} by starting the reaction with increasing amounts of the substrate ATP. It was observed that {P_2W_{17}}, {P_2W_{12}} and {$P_2W_{15}V_3$} reduced the V_{max}, without affecting the K_m, therefore showing the effect of non-competitive inhibition, while {P_2W_{18}} and {P_5W_{30}} affected both, the V_{max} and the K_m, showing a mixed inhibition (Fig. 5, Table 4).

The effects of POTs compounds were also examined in the human neuroblastoma SH-SY5Y cell line to see if they could affect cell viability. However, POTs did not reduced the cell survival at the IC_{50} values (results not shown), on contrary with the effects recently described for gold compounds [48].

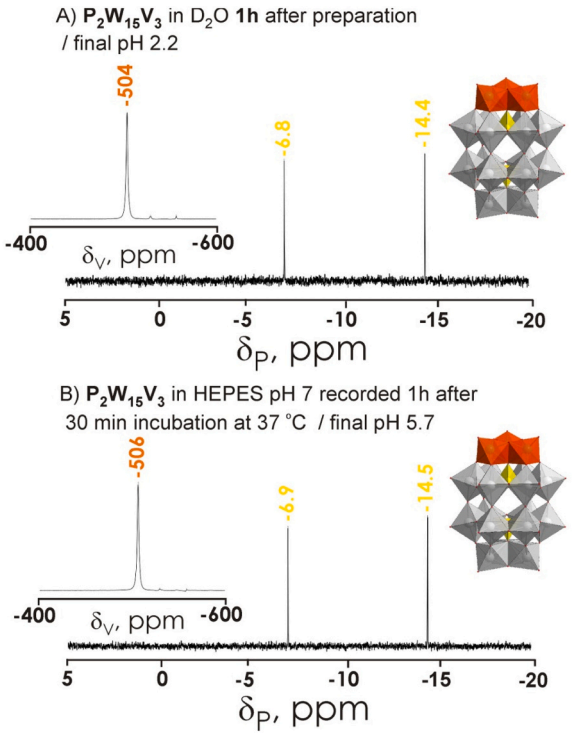

Fig. 7. ^{31}P and ^{51}V (insert) NMR spectra of 1 mM {$P_2W_{15}V_3$} solutions A) in D_2O recorded approximately 1 h after preparation; B) in 25 mM HEPES (pH 7.0), 100 mM KCl, 5 mM $MgCl_2$, 50 μM $CaCl_2$ recorded after incubation for 30 min at 37 °C. The signal at −6.9 to −6.8 and − 14.5 – −14.4 ppm corresponds to 2 non-equivalent P ions in {$P_2W_{15}V_3$} shown in yellow in polyhedral presentation. [30] The ^{51}V shift corresponds to three equivalent V ions shown in orange. [30] Color code: {WO_6}, light grey; {VO_6}, orange; {PO_4}, yellow; O, red. (For interpretation of the references to color in this figure legend, the reader is referred to the web version of this article.)

3.6. NMR stability studies

The importance of POMs' speciation in biological studies, although not usually considered, is of paramount importance for determining the dominant POM species, or combinations thereof, responsible for specific POM activity [49]. Herein, the speciation of the respective POTs in enzymatic test medium at pH 7.0 (25 mM HEPES pH 7.0, 100 mM KCl, 5 mM $MgCl_2$, 50 μM $CaCl_2$) after incubation for 30 min at 37 °C and in water is performed by ^{31}P and ^{51}V NMR analysis to address cluster species responsible for interaction in solution. After dissolving the most promising SERCA Ca^{2+}-ATPase inhibitor {P_5W_{30}} in H_2O (Fig. 6A) or HEPES pH 7.0 buffer (Fig. 6B), only the intact Preyssler anion has been detected in solution. In an aqueous solution of {P_2W_{18}}, only the intact Wells-Dawson $[P_2W_{18}O_{62}]^{6-}$ anion was detected (Fig. S2A), which, however, was partially hydrolyzed to the monolacunary form $[P_2W_{17}O_{61}]^{10-}$ in enzymatic assay medium (Fig. S2B). The mixed-metal vanadium-substituted Wells-Dawson anion {$P_2W_{15}V_3$} is stable both in water (Fig. 7A) and HEPES pH 7.0 (Fig. 7B) as confirmed by ^{31}P and ^{51}V NMR spectroscopy. ^{31}P NMR analysis of spectra recorded from {P_2W_{17}} and {P_2W_{15}} solutions in water and in HEPES buffer showed that monolacunary anions are predominant (Fig. S3-S4). The ^{31}P NMR spectra of hexalacunary POT {P_2W_{15}} (Fig. S5) points to the presence of a low amount of unhydrolyzed hexalacunary anion $[H_2P_2W_{12}O_{48}]^{12-}$ together with monolacunary anion $[\alpha_2\text{-}P_2^VW_{17}^{VI}O_{61}]^{10-}$ and $[P_2^VW_{19}^{VI}O_{69}(H_2O)]^{14-}$ anion, which contains two A-α-$[P^VW_9^{VI}O_{34}]^{9-}$ halves linked via one W ion in the equatorial plane and was previously reported as an intermediate species in phosphotungstate solutions [50].

The charge densities for Wells-Dawson clusters were calculated as the ratio between the POT charge q and the number of tungsten atoms *m*

and summarized in Table 1. For the mono-lacunary Wells-Dawson anion $[P_2W_{17}O_{61}]^{10-}$, which is the main species in $\{P_2W_{17}\}$ and $\{P_2W_{15}\}$ systems (Fig. S3-S4), protonation to $H_3[P_2^VW_{17}^{VI}O_{61}]^{7-}$ has been reported [51], resulting in a considerable decrease of the POT charge density $q/m = 0.41$. The different activity for $\{P_2W_{17}\}$ and $\{P_2W_{15}\}$ can be explained by different amounts of $H_3[P_2^VW_{17}^{VI}O_{61}]^{7-}$ in solution, as well as the possible presence of some isopolytungstates as rearrangement byproducts that cannot be detected by ^{31}P NMR spectroscopy. Two intact Wells-Dawson anions $[P_2W_{18}O_{62}]^{6-}$ and $[H_3P_2W_{15}V_3O_{62}]^{6-}$ have the same q/m value of 0.33, but behave slightly differently due to the presence of substituting V ions, which change the charge distribution and, maybe a binding mode as well. The Preyssler-type anion has a comparable charge density of $q/m = 0.46$, showing the highest activity ($IC_{50} = 0.37$ μM) against Ca^{2+}-ATPases in this research, and the previously tested $[H_{10}Se_2W_{29}O_{103}]^{14-}$ anion with $q/m = 0.48$ is the most potent POT inhibitor so far ($IC_{50} = 0.3$ μM). Recent reports on POMs as superchaotrops, showing that POMs with intermediate charge density ($q/m \sim 0.4$) interact considerably strong with various surfaces of different or mixed polarities as presented by a protein molecule [52], support our findings.

Although strong POTs interactions do not equal to strong inhibition, it is understandable that further discussion on this topic will require the charge density calculations of others POMs for comparison. However, recent studies indicate that, for example, $\{V_{10}\}$ electrostatic interactions play at least partial a potential role at least in part, in interfering with SARS-CoV-2 infectivity cycle [53], whereas metformin-decavanadate has IC_{50} SERCA ATPase inhibition value 6 times higher than $\{V_{10}\}$ alone [54]. Further studies are needed to unravel at molecular level why POTs showed stronger inhibitory effect on PMCA Ca^{2+}-ATPase activity than SERCA, as previously described for the interaction of decaniobate and decavanadate with actin [55].

4. Conclusions

In the present study, we further explore the potential of others POTs and POVs as SERCA Ca^{2+}-ATPase inhibitors [21,22], and we examine, for the first time, the effects of several POTs in the PMCA Ca^{2+}-ATPase activity. In addition, here we compare the effects of POTs on two calcium ATPases localized in different places of the cell and from different sources, namely muscle SERCA Ca^{2+}-ATPase and brain PMCA Ca^{2+}-ATPase. SERCA Ca^{2+}-ATPase activity is inhibited by $\{P_5W_{30}\}$, with the $IC_{50} = 0.3$ μM. This is approximately 3 to 4 times lower than the IC_{50} values found for the others three POTs, $\{P_2W_{17}\}$, $\{P_2W_{15}\}$ and $\{P_2W_{15}V_3\}$ in SERCA studies. Similarly, as described before for $[\alpha\text{-}P_2W_{18}O_{62}]^{6-}$ and $[TeW_6O_{24}]^{6-}$ a mixed type of inhibition was observed for $\{P_5W_{30}\}$, $\{P_2W_{17}\}$ and $\{P_2W_{15}\}$. The $\{P_2W_{15}V_3\}$ type of inhibition suggests a different mode of interaction with the Ca^{2+}-ATPase as the kinetic parameters indicate a non-competitive inhibitor, as described before for $\{V_{10}\}$ and $\{Nb_{10}\}$. The different POTs tested showed higher inhibitory activity against brain PMCA Ca^{2+}-ATPase in comparison to muscle SERCA Ca^{2+}-ATPase inhibition, with the IC_{50} values between 0.1 and 0.3 μM for all the 5 POTs tested in PMCA Ca^{2+}-ATPase inhibition. In fact, lower IC_{50} inhibitory values for SERCA and PMCA Ca^{2+}-ATPases were found for the studied POTs, in comparison to others metals compounds and clinical drugs described as Ca^{2+}-ATPase inhibitors [39–47]. NMR stabiblity studies in HEPES (pH 7) buffer indicate that one of the most promising Ca^{2+}-ATPase inhibitor the Preyssler-type $\{P_5W_{30}\}$ is intact under these conditions. Therefore, these compounds may provide new potential tools to selectively inhibits SERCA and/or PMCA in neurons as described recently for gold compounds [48]. However, there is still a need for the availability of specific PMCA inhibitors of relatively low toxicity to mammalian cells that can potentially be used in cell cultures.

Declaration of Competing Interest

The authors declare that they have no known competing financial interests or personal relationships that could have appeared to influence the work reported in this paper.

Data availability

The data that has been used is confidential.

Acknowledgments

This study received Portuguese national funds from FCT - Foundation for Science and Technology through projects UIDB/04326/2020, and LA/P/0101/2020 (M.A.); the Austrian Science Fund (FWF): P33927 (N.G.); P33089 (A.R.); the University of Vienna (N.G. and A.R.); Projects BFU2017-85723-P (to A.M.M. and C.G-M), and PID2020-115512GB-I00 (to A.M.M.) funded by MCIN/ AEI/ 10.13039/501100011033 and by "ESF Investing in your future".

Appendix A. Supplementary data

Supplementary data to this article can be found online at https://doi.org/10.1016/j.jinorgbio.2022.111952.

References

[1] M.T. Pope, Heteropoly and Isopoly Oxometalates, Springer-Verlag, New York, 1983.
[2] B. Hasenknopf, Polyoxometalates: introduction to a class of inorganic compounds and their biomedical applications, Front. Biosci. 10 (2005) 275–287, https://doi.org/10.2741/1527.
[3] M. Stuckart, K.Y. Monakhov, Polyoxometalates as components of supramolecular assemblies, Chem. Sci. 10 (2019) 4364–4376, https://doi.org/10.1039/c9sc00979e.
[4] L.S. Van Rompuy, T.N. Parac-Vogt, Interactions between polyoxometalates and biological systems: from drug design to artificial enzymes, Curr. Opin. Biotechnol. 58 (2019) 92–99, https://doi.org/10.1016/j.copbio.2018.11.013.
[5] E. Sanchez-Lara, S. Trevino, B.L. Sanchez-Gaytan, E. Sanchez-Mora, M.E. Castro, F. J. Melendez-Bustamante, M.A. Mendez-Rojas, E. Gonzalez-Vergara, Decavanadate salts of cytosine and metformin: a combined experimental-theoretical study of potential metallodrugs against diabetes and cancer, Front. Chem. 6 (2018) 402, https://doi.org/10.3389/fchem.2018.00402.
[6] A. Bijelic, M. Aureliano, A. Rompel, The antibacterial activity of polyoxometalates: structures, antibiotic effects and future perspectives, Chem. Commun. 54 (2018) 1153–1169, https://doi.org/10.1039/c7cc07549a.
[7] A. Bijelic, M. Aureliano, A. Rompel, Polyoxometalates as potential next-generation metallodrugs in the combat against cancer, Angew. Chem. Int. Ed. 58 (2019) 2980–2999, https://doi.org/10.1002/anie.201803868. Angew. Chem. 131 (2019) 3008-3029, http://doi.org/10.1002/ange.201803868.
[8] M. Aureliano, N.I. Gumerova, G. Sciortinod, E. Garribba, A. Rompel, D.C. Crans, Polyoxovanadates with emerging biomedical activities, Coord. Chem. Rev. 447 (2021) 214143, https://doi.org/10.1016/j.ccr.2021.214143.
[9] M. Aureliano, The future is bright for polyoxometalates, BioChem 2 (2022) 8–26, https://doi.org/10.3390/biochem2010002.
[10] C. Pimpão, I.V. da Silva, A.F. Mósca, J.O. Pinho, M.M. Gaspar, N.I. Gumerova, A. Rompel, M. Aureliano, G. Soveral, The aquaporin-3 inhibiting potential of polyoxotungstates, Int. J. Mol. Sci. 21 (2020) E2467, https://doi.org/10.3390/ijms21072467.
[11] R. Raza, A. Matin, S. Sarwar, M. Barsukova-Stuckart, M. Ibrahim, U. Kortz, J. Iqbal, Polyoxometalates as potent and selective inhibitors of alkaline phosphatases with profound anticancer and amoebicidal activities, Dalton Trans. 41 (2012) 14329–14336, https://doi.org/10.1039/c2dt31784b.
[12] J. Breibeck, N.I. Gumerova, B.B. Boesen, M.S. Galanski, A. Rompel, Keggin-type polyoxotungstates as mushroom tyrosinase inhibitors - a speciation study, Sci. Rep. 9 (2019) 5183, https://doi.org/10.1038/s41598-019-41261-7.
[13] G. Chi, L. Wang, B. Chen, J. Li, J. Hu, S. Liu, M. Zhao, X. Ding, Y. Li, Polyoxometalates: study of inhibitory kinetics and mechanism against alpha-glucosidase, J. Inorg. Biochem. 199 (2019), 110784, https://doi.org/10.1016/j.jinorgbio.2019.110784.
[14] M.B. Čolović, D.V. Bajuk-Bogdanović, N.S. Avramović, I.D. Holclajtner-Antunović, N.S. Bošnjaković-Pavlović, V.M. Vasić, D.Z. Krstić, Inhibition of rat synaptic membrane Na^+/K^+-ATPase and ecto-nucleoside triphosphate diphosphohydrolases by 12-tungstosilicic and 12-tungstophosphoric acid, Bioorg. Med. Chem. 19 (2011) 7063–7069, https://doi.org/10.1016/j.bmc.2011.10.008.
[15] L. Yatime, M.J. Buch-Pedersen, M. Musgaard, J.P. Morth, A.-M.L. Winther, B. P. Pedersen, C. Olesen, J.P. Andersen, B. Vilsen, B. Schiøtt, M.G. Palmgren, J. V. Møller, P. Nissen, N. Fedosova, P-type ATPases as drug targets: tools for

medicine and science, Biochim. Biophys. Acta Bioenerg. 1787 (2009) 207–220, https://doi.org/10.1016/j.bbabio.2008.12.019.
[16] M. Aureliano, N.I. Gumerova, G. Sciortino, E. Garribba, C.C. McLauchlan, A. Rompel, D.C. Crans, Polyoxidovanadates' interactions with proteins: an overview, Coord. Chem. Rev. 454 (2022), 214344, https://doi.org/10.1016/j.ccr.2021.214344.
[17] M. Aureliano, V.M.C. Madeira, Interactions of vanadate oligomers with sarcoplasmic reticulum Ca^{2+}-ATPase, Biochim. Biophys. Acta, Mol. Cell Res. 1221 (1994) 259–271, https://doi.org/10.1016/0167-4889(94)90249-6.
[18] M. Aureliano, V.M.C. Madeira, Vanadate oligoanions interact with the proton ejection by the Ca^{2+} pump of sarcoplasmic reticulum, Biochem. Biophys. Res. Commun. 205 (1994) 161–167, https://doi.org/10.1006/bbrc.1994.2644.
[19] M. Aureliano, D.C. Crans, Decavanadate ($V_{10}O_{28}^{6-}$) and oxovanadates: oxometalates with many biological activities, J. Inorg. Biochem. 103 (2009) 536–546, https://doi.org/10.1016/j.jinorgbio.2008.11.010.
[20] G. Fraqueza, C.A. Ohlin, W.H. Casey, M. Aureliano, Sarcoplasmic reticulum calcium ATPase interactions with decaniobate, decavanadate, vanadate, tungstate and molybdate, J. Inorg. Biochem. 107 (2012) 82–89, https://doi.org/10.1016/j.jinorgbio.2011.10.010.
[21] N. Gumerova, L. Krivosudsky, G. Fraqueza, J. Breibeck, E. Al-Sayed, E. Tanuhadi, A. Bijelic, J. Fuentes, M. Aureliano, A. Rompel, The P-type ATPase inhibiting potential of polyoxotungstates, Metallomics 10 (2018) 287–295, https://doi.org/10.1039/c7mt00279c.
[22] G. Fraqueza, J. Fuentes, L. Krivosudsky, S. Dutta, S.S. Mal, A. Roller, G. Giester, A. Rompel, M. Aureliano, Inhibition of Na(+)/K(+)- and Ca(2+)-ATPase activities by phosphotetradecavanadate, J. Inorg. Biochem. 197 (2019), 110700, https://doi.org/10.1016/j.jinorgbio.2019.110700.
[23] M. Aureliano, G. Fraqueza, C.A. Ohlin, Ion pumps as biological targets for decavanadate, Dalton Trans. 42 (2013) 11770–11777, https://doi.org/10.1039/C3DT50462J.
[24] D. Althumairy, K. Postal, B.G. Barisas, G.G. Nunes, D.A. Roess, D.C. Crans, Polyoxometalates function as indirect activators of a G protein-coupled receptor, Metallomics 12 (2020) 1044–1061, https://doi.org/10.1039/D0MT00044B.
[25] B. Dawson, The structure of the 9(18)-heteropoly anion in potassium 9(18)-tungstophosphate, $K_6(P_2W_{18}O_{62})\cdot 14H_2O$, Acta Crystallogr. 6 (1953) 113–126, https://doi.org/10.1107/S0365110X53000466.
[26] R. Contant, W. Klemperer, O. Yaghi, Potassium octadecatungstodiphosphates (V) and related lacunary compounds, in: A.P. Ginsberg (Ed.), Inorganic Syntheses, John Wiley & Sons, Inc., New York, 2007, pp. 104–111.
[27] A. Müller, V.P. Fedin, C. Kuhlmann, H.-D. Fenske, G. Baum, H. Bögge, B. Hauptfleisch, 'Adding' stable functional complementary, nucleophilic and electrophilic clusters: a synthetic route to $[\{(SiW_{11}O_{39})Mo_3S_4(H_2O)_3(\mu\text{-}OH)\}_2]_{102}$ and $[\{(P_2W_{17}O_{61})Mo_3S_4(H_2O)_3(\mu\text{-}OH)\}_2]_{142}$ as examples, Chem. Commun. 13 (1999) 1189–1190, https://doi.org/10.1039/A903170G.
[28] R.G. Finke, D.K. Lyon, K. Nomiya, T.J.R. Weakley, Structure of nonasodium – triniobatopentadecawolframatodiphosphate-acetonitrile-water (1/2/23), $Na_9[P_2W_{15}Nb_3O_{62}]\cdot 2CH_3CN\ 23H_2O$, Acta Cryst. C46 (1990) 1592–1596, https://doi.org/10.1107/S0108270190000038.
[29] S.S. Mal, U. Kortz, The wheel-shaped Cu_{20} tungstophosphate $[Cu_{20}Cl(OH)_{24}(H_2O)_{12}(P_8W_{48}O_{184})]^{25-}$ ion, Angew. Chem. Int. Ed. 24 (2005) 3777–3780, https://doi.org/10.1002/anie.200500682.
[30] R.G. Finke, B. Rapko, R.J. Saxton, P.J. Domaille, Trisubstituted heteropolytungstates as soluble metal oxide analogs. 3^1. synthesis, characterization, ^{31}P, ^{29}Si, ^{51}V, and 1-and 2-D ^{183}W NMR, deprotonation, and proton mobility studies of organic solvent solute forms of $H_xSiW_9V_3O_{40}^{x-7}$ and $H_xP_2W_{15}V_3O_{62}^{x-9}$, J. Am. Chem. Soc. 108 (1986) 2947–2960, https://doi.org/10.1021/ja00271a025.
[31] M.H. Alizadeh, S.P. Harmalker, Y. Jeannin, J. Martin-Frer, M.T. Pope, A Heteropolyanion with fivefold molecular symmetry that contains a nonlabile encapsulated sodium ion. The structure and chemistry of $[NaP_5W_{30}O_{110}]^{14-}$, J. Am. Chem. Soc. 107 (1985) 2662–2669, https://doi.org/10.1021/ja00295a019.
[32] Y. Jeannin, J. Martin-Frere, D.J. Choi, M.T. Pope, The sodium pentaphosphato(V)-triacontatungstate anion isolated as the ammonium salt, in: A.P. Ginsberg (Ed.), Inorganic Syntheses, John Wiley & Sons, Inc., New York, 2007, pp. 115–118.
[33] D. Marques-da-Silva, G. Fraqueza, R. Lagoa, A.A. Vannathan, S.S. Mal, M. Aureliano, Polyoxovanadate inhibition of *Escherichia coli* growth shows a reverse correlation with Ca^{2+}-ATPase inhibition, New J. Chem. 43 (2019) 17577–17587, https://doi.org/10.1039/C9NJ01208G.
[34] M. Aureliano, F. Henao, T. Tiago, R.O. Duarte, J.J.G. Moura, B. Baruah, D.C. Crans, Sarcoplasmic reticulum calcium ATPase is inhibited by organic vanadium coordination compounds: Pyridine-2,6-dicarboxylatodioxovanadium(V), BMOV, and an amavadine analogue, Inorg. Chem. 47 (2008) 5677–5684, https://doi.org/10.1021/ic702405d.
[35] M.M. Bradford, A rapid and sensitive method for the quantitation of microgram quantities of protein utilizing the principle of protein-dye binding, Anal. Biochem. 72 (1976) 248–254, https://doi.org/10.1016/0003-2697(76)90527-3.
[36] J.M. Salvador, A.M. Mata, Purification of the synaptosomal plasma membrane (Ca^{2+} + Mg^{2+})-ATPase from pig brain, Biochem. J. 315 (1996) 183–187, https://doi.org/10.1042/bj3150183.
[37] M. Berrocal, D. Marcos, M.R. Sepúlveda, M. Pérez, J. Ávila, A.M. Mata, Altered Ca^{2+} dependence of synaptosomal plasma membrane Ca^{2+}-ATPase in human brain affected by Alzheimer's disease, FASEB J. 23 (2009) 1826–1834, https://doi.org/10.1096/fj.08-121459.
[38] M. Berrocal, I. Corbacho, C. Gutierrez-Merino, A.M. Mata, Methylene blue activates the PMCA activity and cross-interacts with amyloid beta-peptide, blocking Abeta-mediated PMCA inhibition, Neuropharmacology 139 (2018) 163–172, https://doi.org/10.1016/j.neuropharm.2018.07.012.
[39] C. Fonseca, G. Fraqueza, S.A.C. Carabineiro, M. Aureliano, The Ca^{2+}-ATPase inhibition potential of gold (I,III) compounds, Inorganics 8 (2020) 49, https://doi.org/10.3390/inorganics8090049.
[40] I. Moreno, L. Norambuena, D. Maturana, M. Toro, C. Vergara, A. Orellana, A. Zurita-Silva, V.R. Ordenes, AtHMA1 is a thapsigargin-sensitive Ca^{2+}/heavy metal pump, J. Biol. Chem. 283 (2008) 9633–9641, https://doi.org/10.1074/jbc.M800736200.
[41] N.J. Yard, M. Chiesi, H.A. Ball, Effect of cyclopiazonic acid, an inhibitor of sarcoplasmic reticulum Ca^{2+}-ATPase, on the frequency-dependence of the contraction-relaxation cycle of the guinea-pig isolated atrium, Br. J. Pharmacol. 113 (1994) 1001–1007, https://doi.org/10.1111/j.1476-5381.1994.tb17092.x.
[42] J.G. Bilmen, L.L. Wotton, F. Michelangeli, The inhibition of the sarcoplasmic/endoplasmic reticulum Ca^{2+}-ATPase by macrocyclic lactones and cyclosporin A, Biochem. J. 366 (2002) 255–263, https://doi.org/10.1042/bj20020431.
[43] J.G. Bilmen, S.Z. Khan, M.-H. Javed, F. Michelangeli, Inhibition of the SERCA Ca^{2+} pumps by curcumin, Eur. J. Biochem. 268 (2001) 6318–6327, https://doi.org/10.1046/j.0014-2956.2001.02589.x.
[44] S. Grösch, T.J. Maier, S. Schiffmann, G. Geisslinger, Cyclooxygenase-2 (COX-2)–independent anticarcinogenic effects of selective COX-2 inhibitors, JNCI J. Natl. Cancer Inst. 98 (2006) 736–747, https://doi.org/10.1093/jnci/djj206.
[45] J. Palacios, M.R. Sepúlveda, A.M. Mata, Effect of spermine on the activity of synaptosomal plasma membrane Ca^{2+}-ATPase reconstituted in neutral or acidic phospholipids, Biochim. Biophys. Acta Biomembr. 1611 (2003) 197–203, https://doi.org/10.1016/S0005-2736(03)00057-9.
[46] J. Palacios, M.R. Sepúlveda, A.G. Lee, A.M. Mata, Ca^{2+} transport by the synaptosomal plasma membrane Ca^{2+}-ATPase and the effect of thioridazine, Biochemistry 43 (2004) 2353–2358, https://doi.org/10.1021/bi0359473.
[47] A.M. Bondžić, G.V. Janjić, M.D. Dramićanin, L. Messori, L. Massai, T.N. Parac-Vogt, V.M. Vasić, Na/K-ATPase as a target for anticancer metal based drugs: insights into molecular interactions with selected gold(III) complexes, Metallomics 9 (2017) 292–300, https://doi.org/10.1039/C7MT00017K.
[48] M. Berrocal, J.J. Cordoba-Granados, S.A.C. Carabineiro, C. Gutierrez-Merino, M. Aureliano, A.M. Mata, Gold compounds inhibit the Ca^{2+}-ATPase activity of brain PMCA and human neuroblastoma SH-SY5Y cells and decrease cell viability, Metals 11 (2021) 1934, https://doi.org/10.3390/met11121934.
[49] N.I. Gumerova, A. Rompel, Polyoxometalates in solution: speciation under spotlight, Chem. Soc. Rev. 49 (2020) 7568–7601, https://doi.org/10.1039/D0CS00392A.
[50] R.I. Maksimovskaya, G.M. Maksimov, ^{31}P NMR studies of hydrolytic conversions of 12-tungstophosphoric heteropolyacid, Coord. Chem. Rev. 385 (2019) 81–99, https://doi.org/10.1016/j.ccr.2019.01.014.
[51] T. Asakura, L. Donnet, S. Picart, J.-M. Adnet, Extraction of hetero polyanions, $P_2W_{17}O_{61}^{10-}$, $P_2W_{18}O_{62}^{6-}$, $SiW_{11}O_{39}^{8-}$ by TBP, J. Radioanal. Nucl. Chem. 246 (2000) 651–656, https://doi.org/10.1023/A:1006795929703.
[52] A. Solé-Daura, J.M. Poblet, J.J. Carbó, Structure–activity relationships for the affinity of chaotropic polyoxometalate anions towards proteins, Chem. Eur. J. 26 (2020) 5799–5809, https://doi.org/10.1002/chem.201905533.
[53] D. Favre, J.F. Harmon, A. Zhang, M.S. Miller, I.A. Kaltashov, Decavanadate interactions with the elements of the SARS-CoV-2 spike protein highlight the potential role of electrostatics in disrupting the infectivity cycle, J. Inorg. Biochem. 234 (2022), 111899, https://doi.org/10.1016/j.jinorgbio.2022.111899.
[54] A.L. Sousa-Coelho, M. Aureliano, G. Fraqueza, G. Serrão, J. Gonçalves, I. Sánchez-Lombardo, W. Link, B.I. Ferreira, Decavanadate and metformin-decavanadate effects in human melanoma cells, J. Inorg. Biochem. 235 (2022), 111915, https://doi.org/10.1016/j.jinorgbio.2022.111915.
[55] G. Sciortino, M. Aureliano, E. Garribba, Rationalizing the decavanadate(V) and oxidovanadium(IV) binding to G-actin and the competition with Decaniobate(V) and ATP, Inorg. Chem. 60 (2021) 334–344, https://doi.org/10.1021/acs.inorgchem.0c02971.